



**UNITED ARAB REPUBLIC
ATOMIC ENERGY ESTABLISHMENT
REACTOR & NEUTRON PHYSICS DEPARTMENT**

**CONSTRUCTION OF A THREE-CRYSTAL SCINTILLATION
PAIR SPECTROMETER**

A.M. HASSAN
H.M. ABU-ZEID

1970

SCIENTIFIC INFORMATION DIVISION
ATOMIC ENERGY POST OFFICE
CAIRO, U.A.E.

UNITED ARAB REPUBLIC
ATOMIC ENERGY ESTABLISHMENT
REACTOR & NEUTRON PHYSICS DEPARTMENT

CONSTRUCTION OF A THREE-CRYSTAL SCINTILLATION
PAIR SPECTROMETER

BY

A.M. HASSAN

H.M. ABU-ZEID

1970

SCIENTIFIC INFORMATION DIVISION
ATOMIC ENERGY POST OFFICE
CAIRO, U.A.R.

A B S T R A C T

This report deals with the details of the construction and tests of the three crystal scintillation pair spectrometer. It also describes the details of the design and construction of the radiation shield and collimation of the thermal neutron beam. It is found that the intensity of the collimated thermal neutron beam at the target place is 10^6 neutron/cm²sec. The central scintillation head has an energy resolution $\sim 7.5\%$ for the Cs¹³⁷ line of 0.662 MeV, with a NaI(Tl) crystal of dimensions (1.75" ϕ x 2"L). The two sides scintillation heads have a resolution of about 10% for NaI(Tl) crystals with the dimensions (3" ϕ x 3"L). The electronic equipment i.e., a pulse shaper for the fast coincidence input and another for the analyzer gate, a stabilized power supply and the matching cathode followers were locally constructed. The linearity of a (512 pulse Height Analyzer) and the two single P.H.A. was proved. In the fast-slow coincidence circuit, the resolving time used for the fast is about 30×10^{-9} sec., while that of the slow is 0.42×10^{-6} sec. The fast-slow coincidence was checked using Na²² standard source which indicates that the electronic equipments are satisfactory for a three-crystal pair spectrometer. Also in this report, the gamma-ray spectrum following thermal neutron capture in natural lead is taken, as a check for the validity of the spectrometer.

1. PRINCIPLE OF OPERATION

Our crystal spectrometer consists of three NaI(Tl) crystals (A, B and C) as shown in Fig. (1). The spectrometer is operated in such a way that an incident gamma-ray beam is directly received by what is called the center crystal (A). In order to select the pair events among the photoelectric and Compton events, two large (B) and (C) NaI(Tl) crystals ($3''\phi \times 3''L$) were placed on either side of the center crystal ($1.75''\phi \times 2''L$) so that all three were in line.

The annihilation of the positron accompanying the pair event in the center crystal gave two 0.511 MeV quanta going out in opposite directions which could then be detected in the side crystals. A triple coincidence between the three crystals was considered sufficient to indicate a pair event in the central crystal.

To eliminate the large low energy background from multiple scattering and double Compton effect, a differential pulse height analyser is used with each of the side crystals, so as to admit only the photo-peak of 0.511 MeV. Hence a pulse height analysis of a measured pair spectrum will be of an energy less than the energy of incident gamma radiation by an amount equal to the annihilation energy (1.022 MeV).

2. GEOMETRY OF INCIDENT GAMMA-RAYS ON THE CENTER CRYSTAL

The present work represents part of a program of investigations of gamma-gamma coincidence from gamma-ray cascades following neutrons capture. The coincidence conditions require that the two counters subtend large solid angles with the source. A suitable geometry can only be attained for a target in an external neutron beam. It was decided to measure coincidences between high energy gamma-rays detected by the three crystal pair spectrometer and lower energy gamma-rays detected by a single NaI(Tl) crystal ($3''\phi \times 3''L$). The use of a pair spectrometer in the coincidence measurement had the advantage that only one peak is

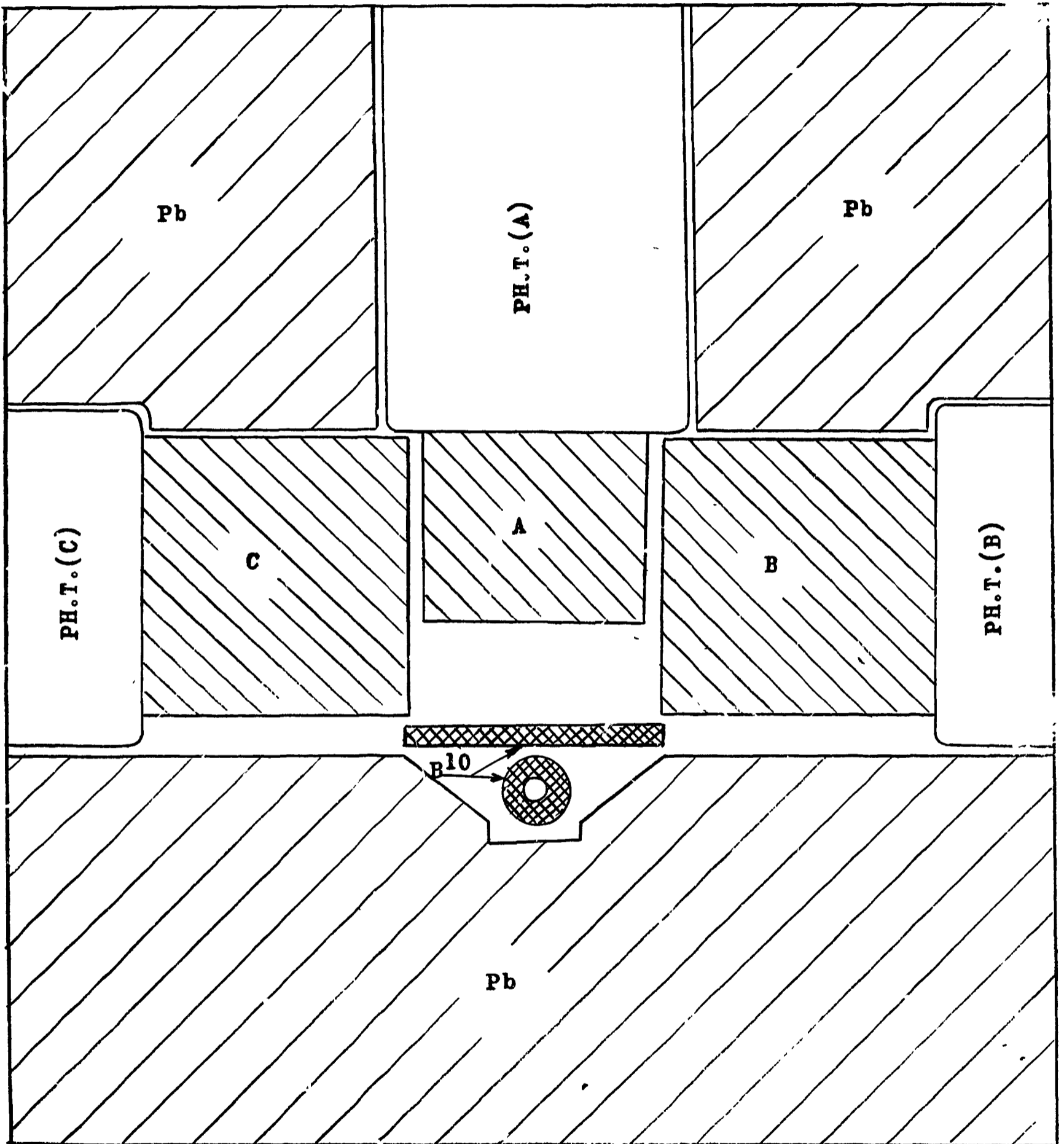


Fig. (1): Crystals Arrangement in Pair Crystal Spectrometer.

present in the spectrum for each gamma-ray. Thus the spectrum of gamma-ray coincident with a given pair spectrometer peak represents in effect the pattern of de-excitation of the particular level populated by high energy gamma-rays.

Thus the pair spectrometer has to be placed very close to the target in order to increase the solid angle (~ 2 steradian). Hence the over all efficiency of this arrangement has nearly the same value as when the sample was placed inside the reactor.

3. ENERGY RANGE

The pair crystal spectrometer can detect gamma-ray energy greater than 1.022 MeV. But the upper limit of the linear part of the energy calibration for the pair spectrometer depends upon the dimensions of the center crystal as well as upon the photomultiplier tube characteristics. The dimensions of the center crystal was chosen in such a way that the electrons of the pairs have a good chance to be stopped in the crystal, and to allow the escape of the annihilation quanta to the side crystals achieving the maximum possible counting efficiency.

In general, as a result of the rapid increase in the pair production cross-section in the central crystal with the incident gamma-ray energy, the present pair spectrometer detection efficiency was found to be rapidly increasing from $\sim 10^{-3}$ at 1.5 MeV to $\sim 2 \times 10^{-2}$ at 10 MeV⁽¹⁾.

4. THE SCINTILLATION HEADS

Several (RCA 6342 A) photo-multiplier tubes and commercial (HARSHAW) NaI(Tl) crystals were tested in order to find an optimum combination.

Criteria used for judging quality were the resolution and the peak-to-valley ratio of the single crystal pulse height spectrum of the (0.662 MeV) gamma-rays from (Cs¹³⁷).

Resolution is defined as the ratio of peak width at half maximum to the pulse height at the center of the peak. The peak-to-valley ratio in

the pulse height spectra is the ratio of the counts/channel at the central position of the peak to the counts/channel at the center of the adjacent valley.

The schematic diagram of the cathode follower associating the photo-multiplier tube in each scintillation head is shown in Fig. (2). It was constructed and used to test the photo-multiplier tubes and the crystals. With a particular (RCA 6342A) photo-multiplier tube, eight crystals were bench tested. Also for each crystal, eight photo-multiplier tubes were bench tested. The dimensions of crystals used are :

(2.25"φx1.75"L, 2"φx2"L, 1.75"φx2"L and 3"φx3"L).

In case of crystals having dimensions (2.25"φx1.75"L, 1.75"φx2"L and 3"φx3"L) a coupling plexiglass light guides with conical sides, were put between crystals and photo-tube, after good poleering. In the second case in which the dimensions of crystals 2"φx2"L there is no light guides because the diameter of the photo-tube is similar to the diameter of the crystal itself. In both cases, silicon oil was used to provide good optical coupling.

The photomultiplier tube and the potential divider were arranged and connected together inside a cylindrical aluminium can ending with an aluminium box inside which was built the cathode follower shown in Fig. (2). The photo-multiplier tube was surrounded by μ -metal tube for good magnetic shielding. The crystal was fixed tightly on the photo-tube by the help of one of the cover of the cylindrical cans which contained a suitable hole-backed with rubber ring-through which the crystal passed. The output plug from the cathode follower and the high voltage plugs were fixed on one side of the aluminium box at the end of the cans. The aluminium box which contain the cathode follower and potential divider was tightly fixed with the cylindrical aluminium can by screwed copper ring. The potential divider of the photo-tube which is shown in Fig. (2) and the interdynode potential were adjusted to give the best resolution.

The output from the cathode follower of the photomultiplier crystal system was fed into a Russian linear amplifier type No. TNII-TC-3199, 1964, the output of which was fed to the input of 512 pulse height analyser. With such a set-up, it was possible to detect the effect of the interdynode potential on the resolution of the photo-peak from Cs^{137} standard source.

The focussing electrode, potential was adjusted to achieve an optimum resolution.

In order to reduce the photo-multiplier noise, the photo-cathode was maintained at the same potential as the crystal. Putting the photo-cathode potential above the ground potential and insulating crystal from the ground would run the risk of developing surface charges on the crystal, thus the mounted crystal was grounded and the photo-cathode was maintained at ground potential by applying the positive high tension to the anode of photo-multiplier tube as shown in Fig. (2).

The following table (1) shows the resolution and the peak-to-valley ratio of single crystal pulse height spectrum of the (0.662 MeV) for the best group of photo-multiplier tube and crystal system selected from the tested group.

Table (1)

Serial No.	Dimensions	Resolution	Peak-to-Valley
1	1.75" ϕ x 2" L	7.5%	20.0
2	2" ϕ x 2" L	7.5%	18.0
3	2.25" ϕ x 1.75" L	8.5%	14.0
4	2.25" ϕ x 1.75" L	9.0%	15.0
5	2.25" ϕ x 1.75" L	9.5%	18.5
6	2.25" ϕ x 1.75" L	8.5%	14.0
7	3" ϕ x 3" L	10.0%	13.0
8	3" ϕ x 3" L	9.5%	14.0

(Harshaw NaI(Tl) crystal with dimensions $1.75''\phi \times 2''L$, was selected for the central crystal which has a resolution 7.5% for Cs^{137} (0.662 MeV). The two side crystals were selected to be larger (Harshaw NaI(Tl) $3''\phi \times 3''L$ diameter, to increase the detection probability of the annihilation quanta ($\sim 14\%$)⁽²⁾ leading to an increase in the efficiency of the spectrometer as a whole.

After selections and initial tests for crystals and their suitable photo-multipliers, the cathode follower connected to the potential divider of each scintillation head was connected as shown in Fig. (2). Such a cathode follower, acts mainly as an impedance matching device where pulses with fast rise time must be transferred through a coaxial cable from one part of the circuit to the other, in addition to the production of high input resistance and low input capacitance required for small pulse rise time. The output of the cathode follower is a negative ~ 0.5 volt. pulse of 5 μ sec. duration which meets the requirements of the amplifiers input.

5. THE EXPERIMENTAL ARRANGEMENT

The UA-RR-1 was used as a source of neutrons for the capture gamma-ray measurements. A collimated beam of neutrons from one of the direct horizontal reactor holes, $60\text{ mm}\phi$ was used to irradiate the sample. The UA-RR-1 is a 2MW, research reactor with 10% enriched Uranium fuel. At this power level, the average thermal neutron flux at the reactor core is $\sim 2 \times 10^{13}$ $n_0/\text{cm}^2 \cdot \text{sec}$. The reactor gamma-ray flux results mainly from the fission process itself, and the neutron capture in the nuclei of the reactor materials. Reduction of these gamma-ray flux at the sample position proved to be more difficult for a hole which looks directly at the core than for a hole which runs tangential to the core.

As a result of lack of such tangential hole in our research reactor we were inforced to use a horizontal hole ($60\text{ mm}\phi$) which directly face the core.

In order to minimise the reactor gamma-ray flux a bismuth plug (200 mm length 60 mm ϕ) was inserted inside the reactor hole (in the shielding zone) in front of the internal collimator from the core side.

Since the shielded crystal pair spectrometer detector is set at an angle 90° to the neutron beam, the core gamma-rays must therefore undergo a Compton scattering to enter the detector. Consequently most of the core gamma-ray reaching the pair detector will have energies much less than 1 MeV, which is below the energy range of the present measurements.

5.1 Neutron Collimation :

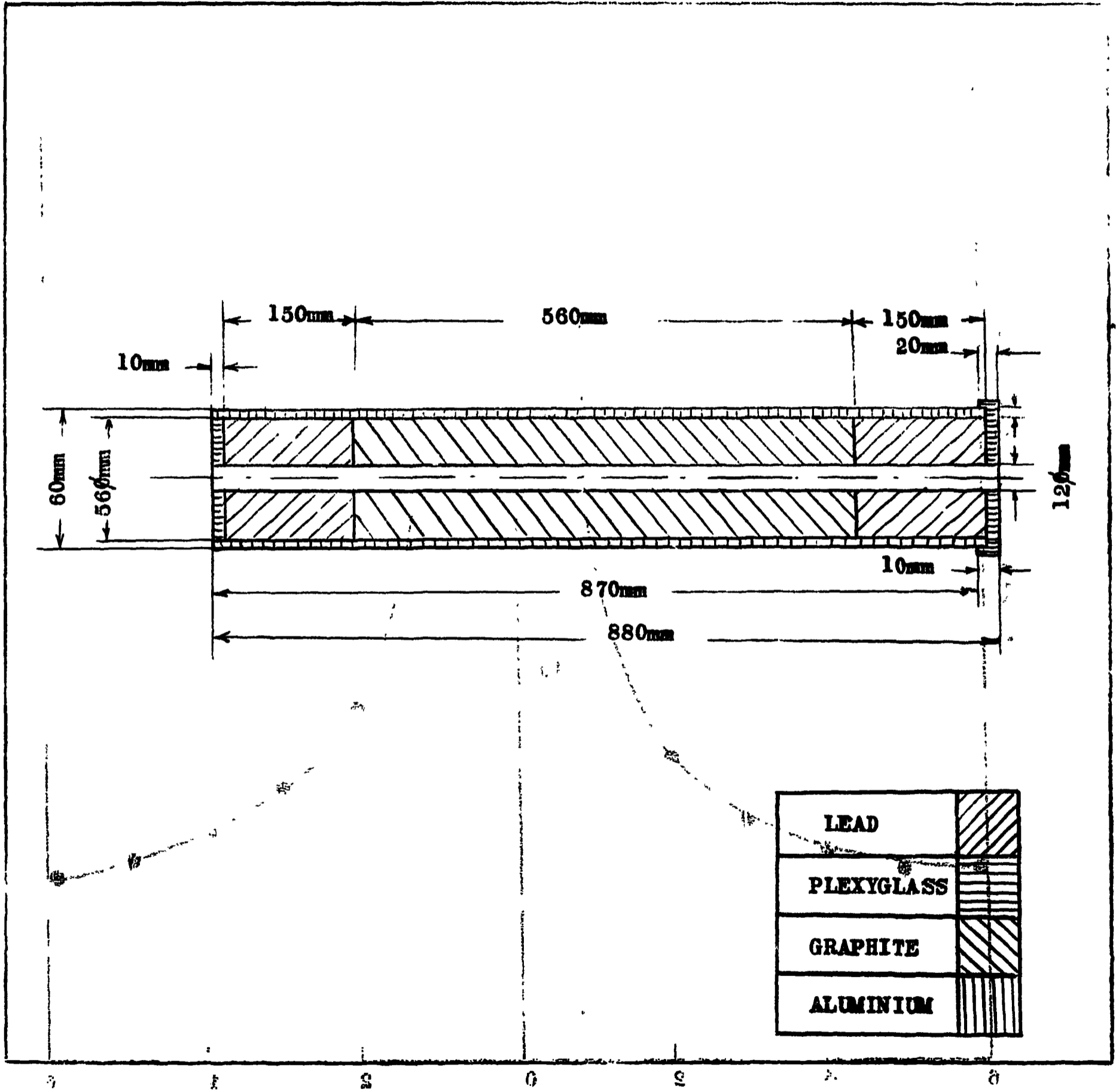
To obtain good quality capture gamma-ray spectra, it is desirable to use a thermal neutron beam having a minimum cross-section area. In this way extraneous back ground counting effects due to scattering of a large diameter beam off the shielding, source holder, beam catcher, etc. ... are minimised. To accomplish this a collimator having (12mm ϕ) hole was constructed and inserted into hole (8). For maximum effectiveness it is necessary to collimate both the epithermal and fast neutrons and the reactor gamma-rays, in addition to the thermal neutrons.

Thus a collimator was constructed as shown in Fig. (3) using graphite and lead. The graphite served to collimate the thermal neutrons and the lead to collimate gamma-rays.

At the target position, after collimation the thermal neutron flux was found to be of the order of 10^6 neutron/cm². Second, measured by the activation of an indium foil. The distribution of the neutron flux along the perpendicular to the neutron beam, at the sample position is shown in Fig. (4).

5.2 Detectors Shield Arrangement :

Figures (1 and 5) show a horizontal and vertical cross-section of the pair spectrometer detector together with its associated shield.



(mm) 560
Fig. (3): Internal Collimator.

Fig. 1: The Distribution of the Neutron Flux at the Target

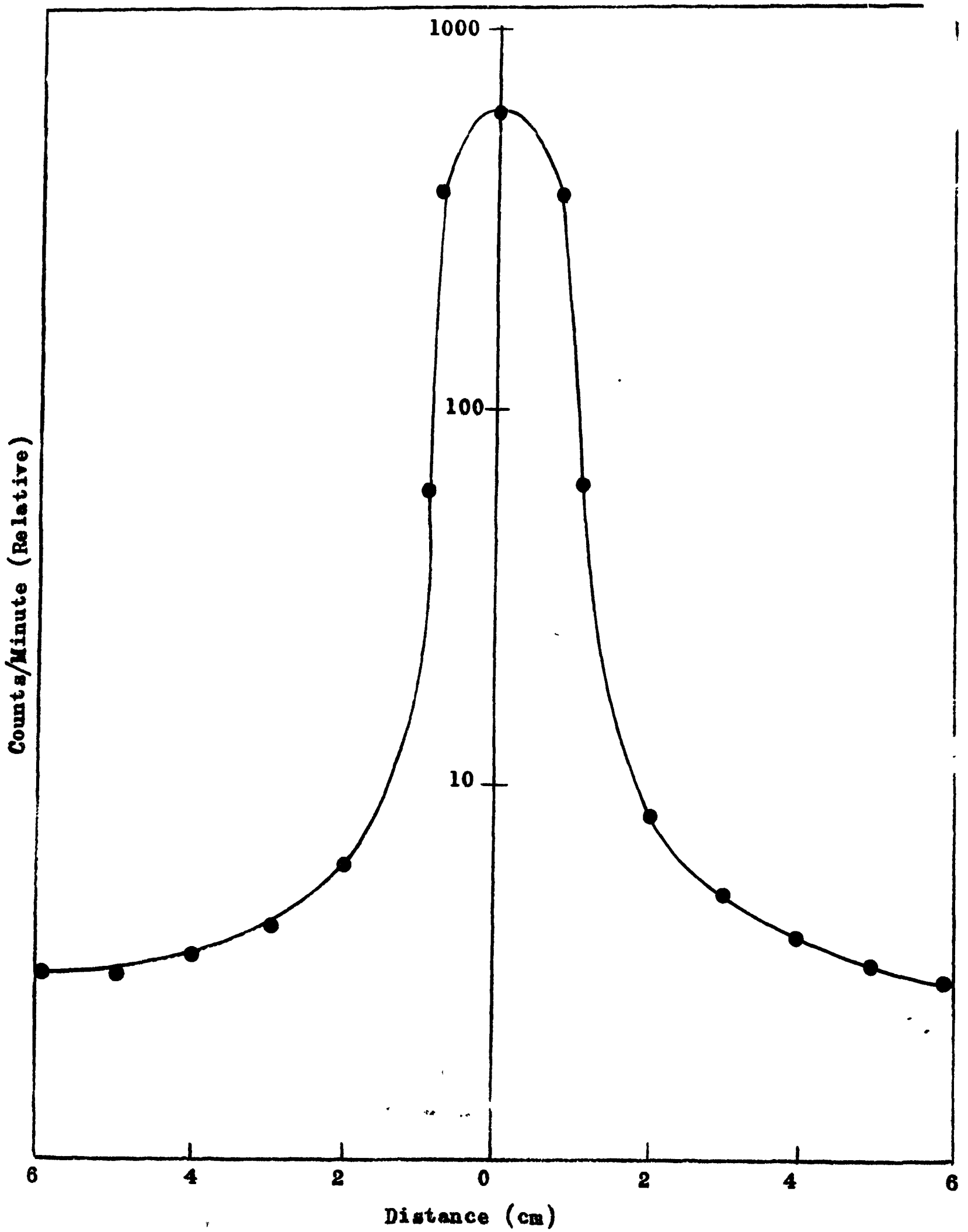


Fig. (4): The Distribution of the Neutron Flux at the Target Place.

The detector shielding consisted of lead (having a minimum thickness of 10 cm) which was, in turn shielded by 10 cm Borated Paraffin (containing 40% boron carbide). In this way thermal neutrons scattered from the beam were prevented from being captured in the lead shield with the resultant emission of 7.38 MeV capture gamma-rays. Instead, such scattered thermal neutrons were absorbed by the boron with the resultant 0.477 MeV prompt gamma-rays from $(B^{10}(n,\alpha)Li^7)$ reaction⁽³⁾ being absorbed by the lead. In the direct path between the sample and the internal collimator there was a hole in the lead shield with a diameter 22 mm.

Since there is an appreciable neutron scattering by a sample, it is necessary to locate a neutron shield in front of the detector.

5.3 Beam Catcher :

It was necessary to completely absorb the external reactor beam in a beam catcher. It is desirable to accomplish this with a minimum production of high energy capture gamma-rays, and a minimum neutron and gamma-ray back scattering into the sample detector area.

Consequently, with beam catcher which was constructed, the neutron beam is led down a (10 cm ϕ , 20 cm long) hole into the central region of Borated Paraffin Block. The Paraffin block is contained in a lead shield 10 cm thick walls as shown in Fig. (5).

6. ELECTRONIC EQUIPMENT SET-UP

A block diagram of electronic circuitry is shown in Fig. (6). The pulses from the cathode follower of center crystal system are amplified by a Russian linear amplifier type (TNII-TC-3199-1964) and fed after 2 μ sec. delay line and matching cathode follower into the input of 512 pulse height analyser.

Each of the side crystals (A) and (B) received annihilation photons from the pair events as well as the scattered gamma-rays, produced by gamma radiation incident on the central crystal (C). These pulses coming

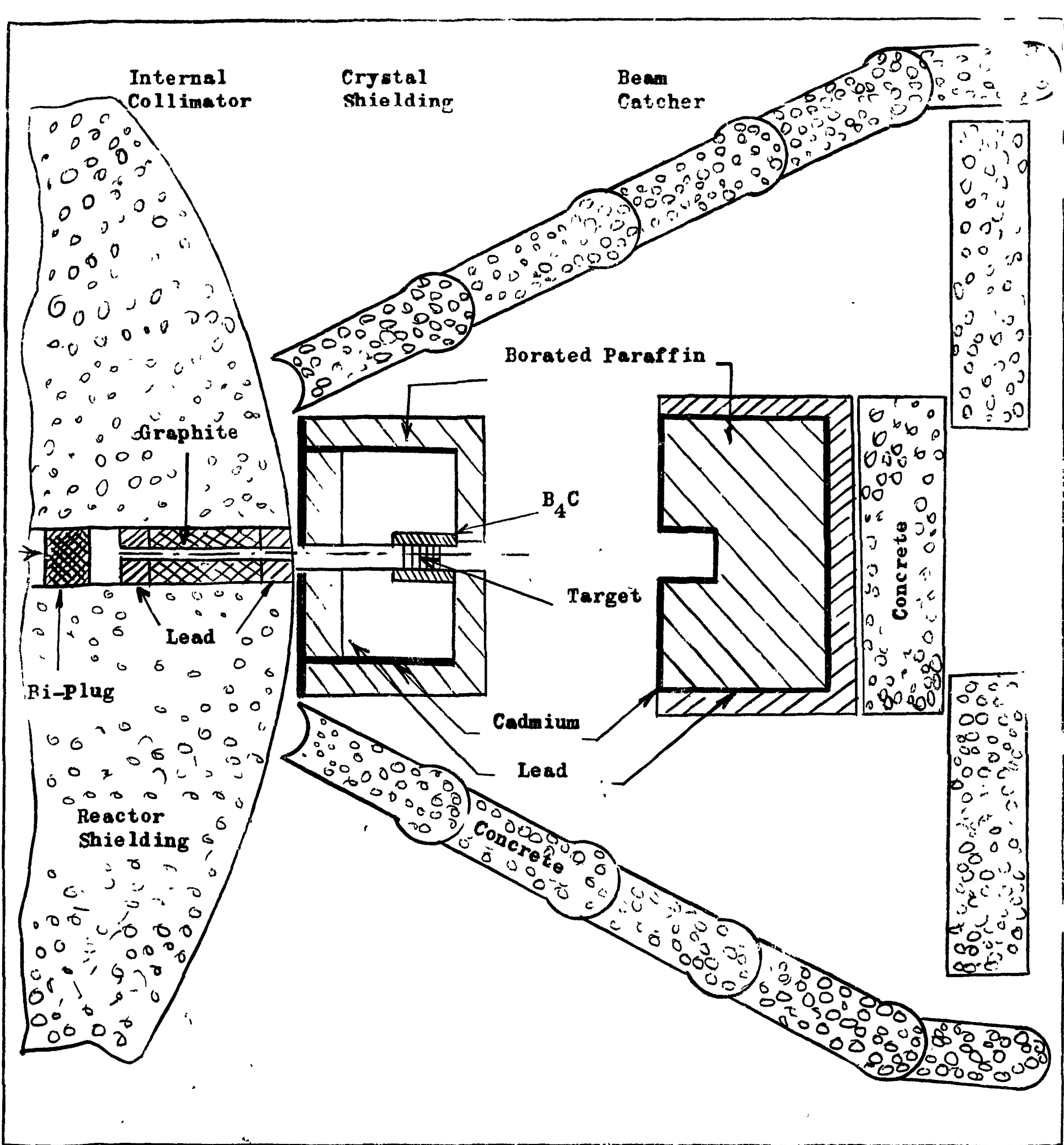


Fig. (5): Schematic Diagram of Shielding Assembly at the Reactor Hole.

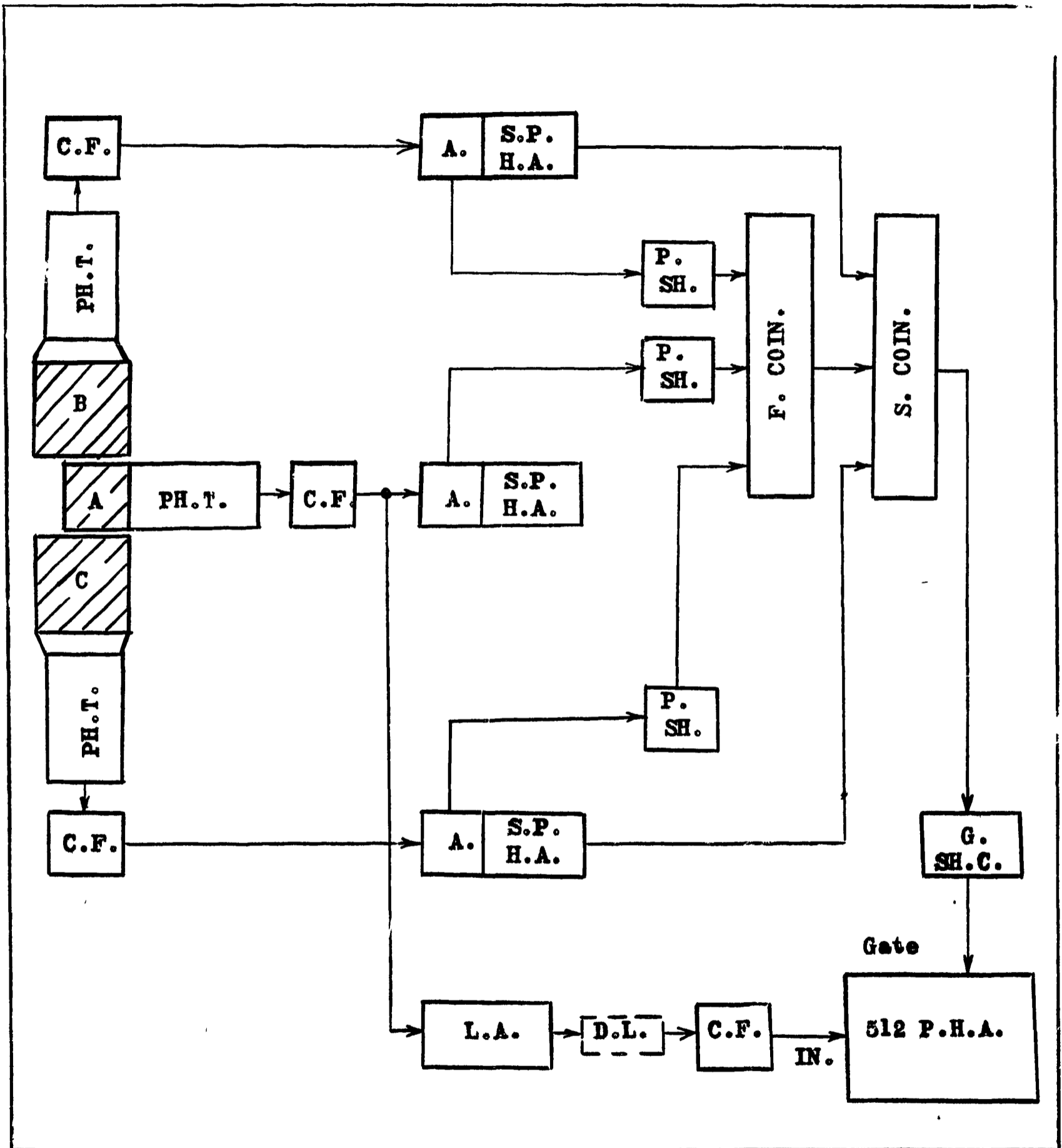


Fig. (6): Block Diagram of the Three Crystal Pair Spectrometer.

from the two side cathode followers were amplified by two-Hamner-linear amplifiers type (N.J.U.S.A. model 328) and fed into the fast coincidence type (101 N.E.H.R. Inc.) through two units of pulse shaper circuits. Also the pulses from the cathode follower of the center crystal amplified by (Hamner) linear amplifier type (N.J.U.S.A. Model 328) were fed into the same fast coincidence through a third unit of pulse shaper.

The pulses from the two side linear amplifiers are fed after two single pulse height analysers into slow coincidence type (1036 A.E.R.E. serial 412). In the same time the pulses coming from the output of the fast coincidence were fed directly into the third unit of the slow coincidence.

At last the output pulses from the slow coincidence were fed after a gated pulse shaper circuit into the linear gate of 512 pulse height analyzer.

Phillips power units type (P.W. 4025) were used to supply the photo-multipliers with stabilized high voltage.

Other stabilized power units used to supply cathode followers were constructed locally.

Some suitable electronic circuits from different references^(4,5,6,7) have been selected and modified in order to suit the required specifications. In this part we shall give a short account about these equipments.

6.1 Single Pulse Height Analysers (S.P.H.A.) :

We used two single pulse height analysers (Hamner type N.J.U.S.A. 328) and by using standard sources of gamma radiations which were :

Na^{22} , Co^{60} , Zn^{65} and Cs^{137} , the linearity of each equipment was found as follows.

An amplisorter was connected with the output of the cathode follower of each side crystal head which was, intern, exposed to standard gamma-ray sources one after the other. The output of the S.P.H.A. was connected to a scaler with timer.

By varying the base drum position (E-volts) while keeping the window drum at constant value $\Delta E=1$ volt, the counts/unit time could be registered for each value of E.

Results of each source were plotted and the photo-peaks amplitude voltages which correspond to their channel number were determined. Knowing the energy for each peak of the standard sources we could plot the relation between the energy in MeV against the number of channels which correspond to the voltage reading at (E) drum.

Both curves showed good linear relation which passed by the origin.

The resolution for the characteristic gamma-rays from the different source were found to be described by the usual relation that the resolution is inversely proportional to the square root of gamma-ray energy.

6.2 Linearity of 512 P.H.A. :

Two methods were used to check the linearity of the 512 P.H.A. One is by means of a precision pulse generator (RIDL Mercury Pulse Gen. Mod. 47-1); which was used to provide pulses of full scale amplitude, half full scale, a quarter of full scale, and so on. With an (R-C) shaping network the pulses from this generator were given the same shape as the pulses from the detector.

By this, the cathode-follower, the Russian linear amplifier (Type TC-3199-64 TNII) and the 512 multi-channel analyser proved to be linear and stable over a long period to within $\pm 1\%$.

In the second method, a rapid indication of the differential linearity of the analyser was obtained by making two measurements of a Cs^{137} at two widely different gain settings. It shows that the spectral shape is the same for both cases and this gives an indication of excellent differential linearity.

6.3 Fast Coincidence :

The fast coincidence unit (model 101 N EH research Lab., Inc.). This model is designed to deliver an output pulse whenever a time coincidence occurs among pulses appearing on all the activated input channels, except when a pulse appears on the anti-input channel.

For this coincidence circuit, sources of negative going pulses (greater than -2V ranging from 0.1 μ sec. to 50 nsec. in width) can be connected into the inputs. In order to avoid major pulse reflections (125 ohm) cable is used. With the more shorting switch (SW6) on (TERM) position the resolution time—the time displacement required to reduce the output amplitude by a significant factor—will be of the order of the input pulse width.

The fast coincidence was tested by the delayed coincidence method⁽⁶⁾ using Co^{60} as standard source of gamma radiation. By inserting a variable delay line in series with one of the two output from the pulse shaper unit, and varying the delay line value we noticed a decrease in the counting rate of the double coincidence unit.

A curve could be plotted of the recorded coincidence rate as a function of artificial delay time inserted in series with each channel. Such a curve is called a prompt resolution curve which will have a rounded shape as shown in Fig. (7). It is worthy to mention that this prompt resolution curve will have a rectangular shape of full width equal to $2\tau_0$ if the counter and the coincidence circuit are ideal, where τ_0 is the resolving time of the fast coincidence circuit.

The resolving time of the coincidence circuit, $2\tau_0$ can be defined as the effective width of the prompt resolution curve, that is the area divided by its maximum height which is approximately equal to the full width of the curve at half maximum.

Thus from Fig. (7) it is seen that the resolving time of the fast coincidence circuit measured $2\tau_0=100$ n sec., i.e. $\tau_0=50$ n sec.

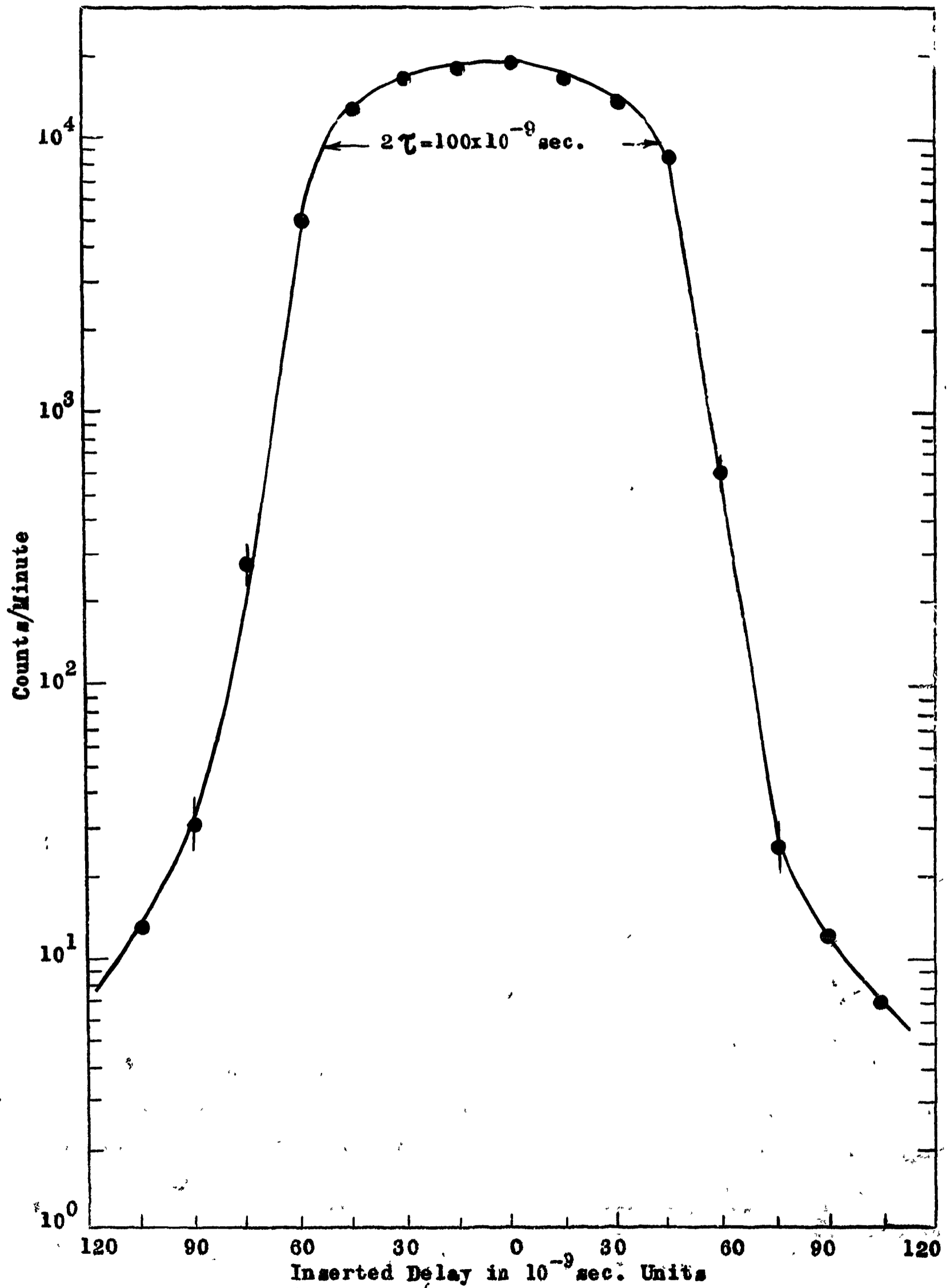


Fig. (7): The Prompt Coincidence Resolution Curve Observed in Testing the Fast Coincidence.

6.4 Slow Coincidence :

The slow coincidence circuit used in the pair spectrometer is (A.E.R.E. Harwell unit, 1036C). It consists of three identical input channels which are provided with amplitude discrimination (range 2 - 20V). Variable paralysis time (5, 10, 200, 300, 400, 500 μ sec.) and variable delay time from (0 to 1 μ sec. in steps of 0.05 μ sec.).

The resolution time of the mixer of the coincidence output channels 1 and 2 with channel 3 may be set to any of the following values (0.1, 0.2, 0.3, 0.4, 0.5, 1, 2 and 4 μ sec.).

The accuracy of the resolution times above is about $\pm 10\%$ but their stability is of order $\pm 2\%$ for times greater than 0.1 μ sec. and $\pm 5\%$ for the shortest resolving time.

In our case the resolving time was set equal to 0.4 μ sec. In order to check this resolving time two independent radioactive sources are used (Cs^{137} and Co^{60}) and counted, the output pulses being fed to channel 1 and 2 of the coincidence unit. The number of input pulses and the number of coincidence in a given time are then measured on three scalars and the resolving time calculated from the following relation⁽⁶⁾

$$N_c = 2 N_1 N_2 \tau$$

where N_c = the average number of coincidence per second,
 N_1 = the average number of input pulses/second in channel No.1,
 N_2 = the average number of input pulses/second in channel No.2,
 τ = the coincidence resolving time in seconds.

Sufficient coincidence pulses had been counted to achieve good statistical accuracy and also it had been noticed that there was no interaction between counters which might give rise to genuine coincidence.

τ = was found experimentally = 0.42 μ sec.

6.5 Construction of a Pulse Shaper :

Our fast coincidence type (101 NEH) needs negative pulses of width ranging from (0.05 μ sec. to 0.1 μ sec. and with amplitude from 3V to 6V). In the same time the amplifiers gives a bipolar pulses with duration about 1.5 μ sec.

A pulse shaper circuit was designed and constructed to connect the amplifier with the fast coincidence circuit. The shaping circuit used is as shown in Fig. (8).

The bipolar signal taken from the amplifier was clipped for a negative part of the pulse with a clipping circuit and applied to the control grid of the univibrator tube (E88CC). The output of such circuit applied to the pentode tube 6X97 which has a negative bias. The final output taken from the anode of the pentode has negative form (with 50 n.sec. width and rise time 20 n.sec.), which is applied to the fast coincidence circuit.

6.6 Construction of a Gate Shaping Circuit :

The coincidence connector terminal of the 512 P.H.A. requires - 3 volts to be held at all time for closing the gate of the analyser which can be opened by a positive pulse with ~2 volts amplitude and ~2.5 μ sec. width.

A suitable pulse shaping circuit was designed as shown in Fig. (9) to open the gate of the 512 P.H.A.

6.7 Construction of a Stabilized Power Supply :

The electronic circuit, shown in Fig. (10) was designed to supply the cathode followers and pulse shaper of our system with the necessary power. At 300 V D.C. of very small ripple component changing from 2 m.V. up to 10 m.V. at maximum load is available. The power transformer was designed to supply the A.C. filament voltage by a separate winding of 6.3 V and 2 A., beside the winding of the voltage supply. Basic design theory of the power supply is covered by Elmore and Sands⁽⁷⁾.

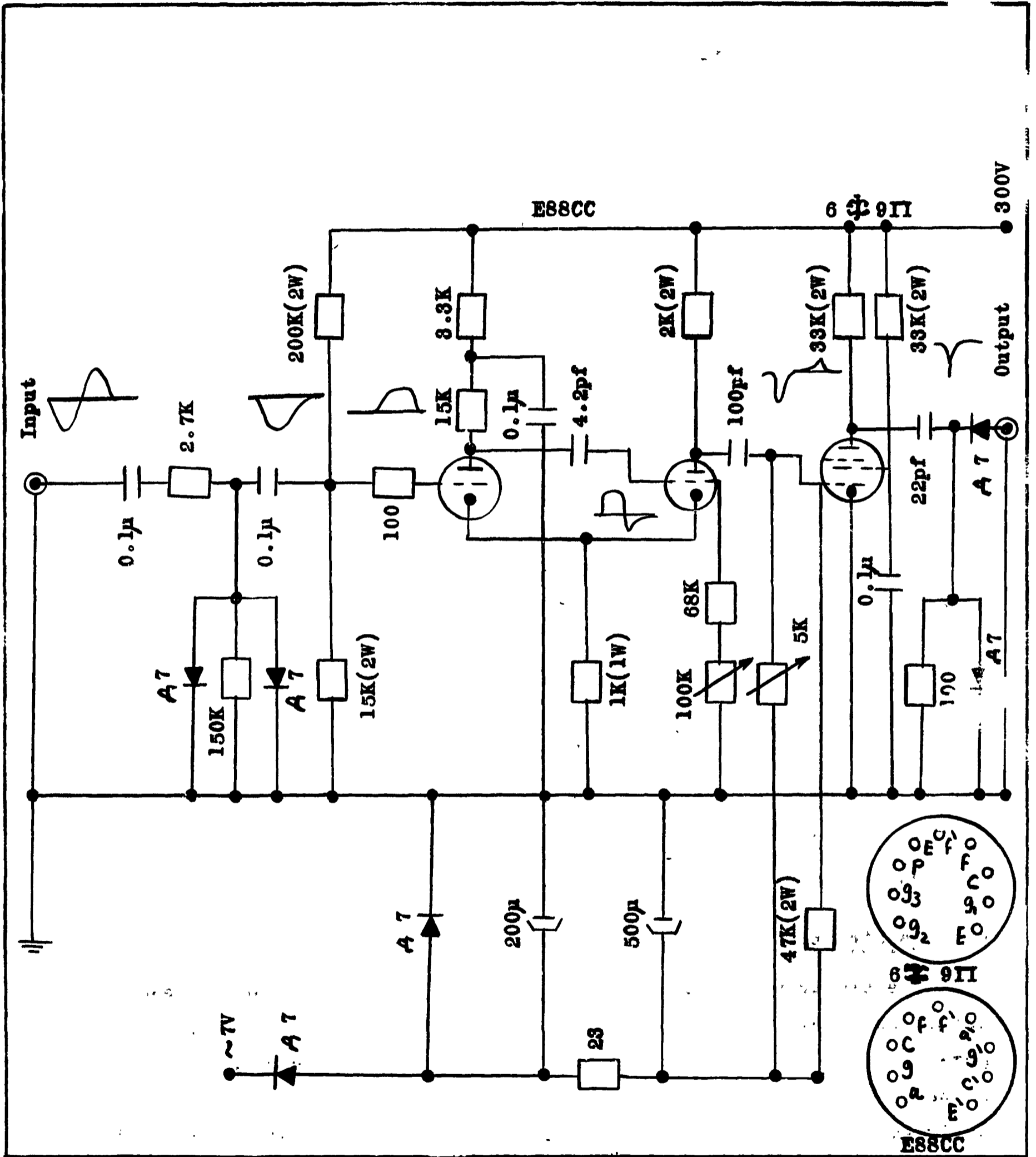


Fig. (8): Pulse Shaper for Coincidence Input.

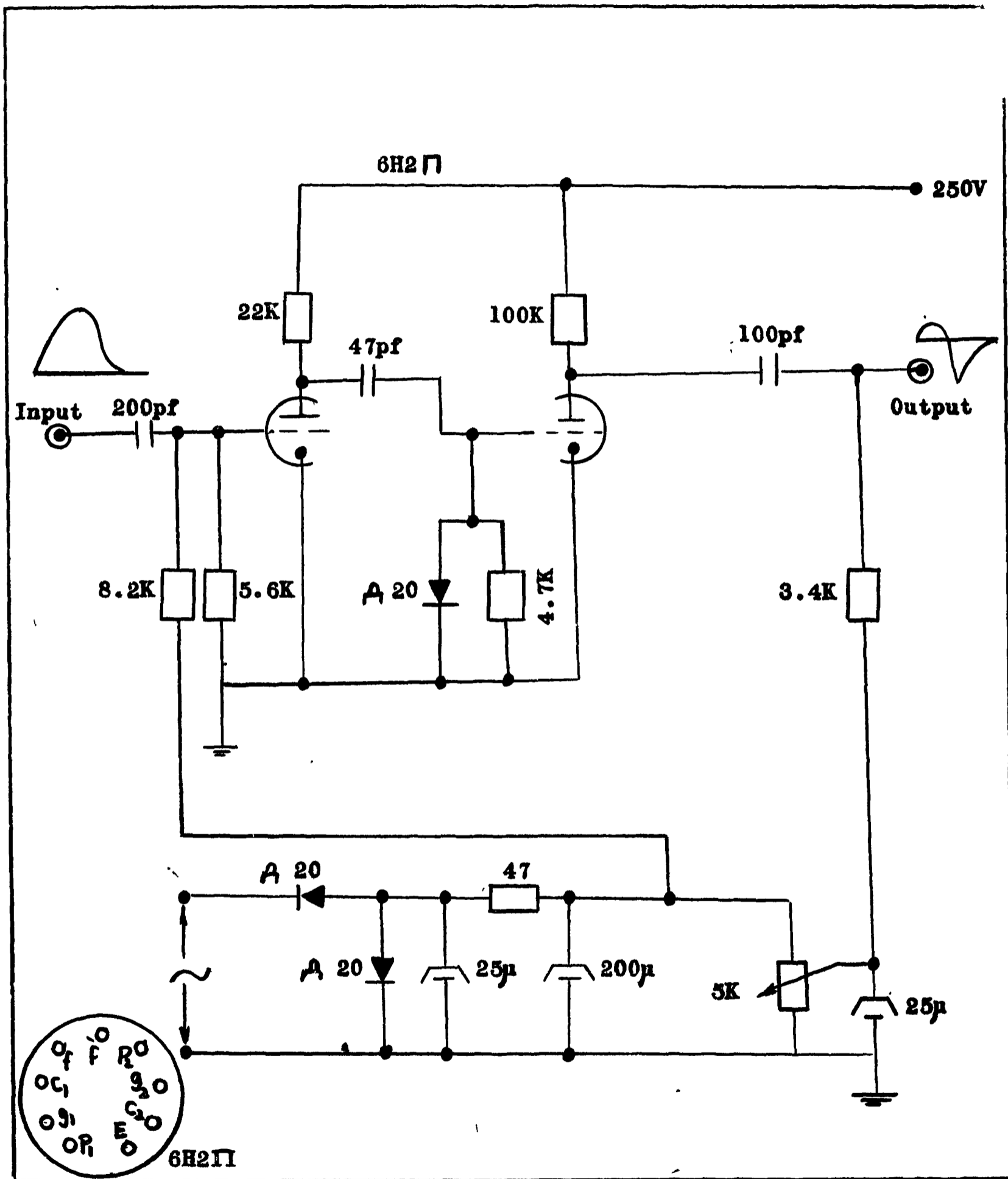


Fig. (9): Gate Shaping Circuit for the Multichannel Pulse Height Analyzer.

Valve 5 U 4 acts as a full wave rectifier and valve (6H5C) acts as a voltage regulator which control the current through the load, its control grid is coupled to the D.C. amplifier (6~~U~~4). The cathode of the tube 6~~U~~4 is connected to the anode of the gas filled tube C Γ 2C which generate a stable voltages of 105 V. at the anode. Valve C Γ 2C acts as the voltage reference tube. The control grid of the valve 6~~U~~4 was connected to the output of the regulated tube through the feed back link R_1 , R_2 and R_3 so that any change in the output voltage give a change at the anode of 6~~U~~4 this change is reversed by 180° which give the reverse of change at the output.

6.8 Construction of a Matching Cathode Follower :

For the coincidence purpose a delay line (D.L.) of the order of $2 \mu\text{sec.}$ was inserted after the main amplifier to the 512 P.H.A.

A cathode follower was constructed as shown in Fig. (11) in order to match the impedance of the D.L. with the impedance of P.H.A. input.

6.9 A Check of the Fast-Slow Coincidence Arrangement :

Fig. (12) shows the arrangement for adjusting and checking the electronic circuit in connection with each side scintillation head. Na^{22} gamma-ray standard source was used for this purpose. In particular the annihilation photo-peak⁽⁸⁾ of energy 0.511 MeV was found useful for adjusting the positions and the widths of the amplisorter window.

Using the previously mentioned calibration curves of the amplisorters, the window width of each of the amplisorters were opened to double width of the full width at half maximum height determined from the resolution curve which is previously mentioned and the base (E) was fixed at $(0.511 - \frac{\Delta E}{2})$. i.e. nearly the total annihilation photo-peak gamma-rays passes through the window of the amplisorter Hamner (N.J.U.S.A.) Model 328).

Fig. (13a) shows the direct spectrum without gating the 512 P.H.A. which give the normal Na^{22} spectrum⁽⁸⁾. Fig. (13b) shows the spectrum

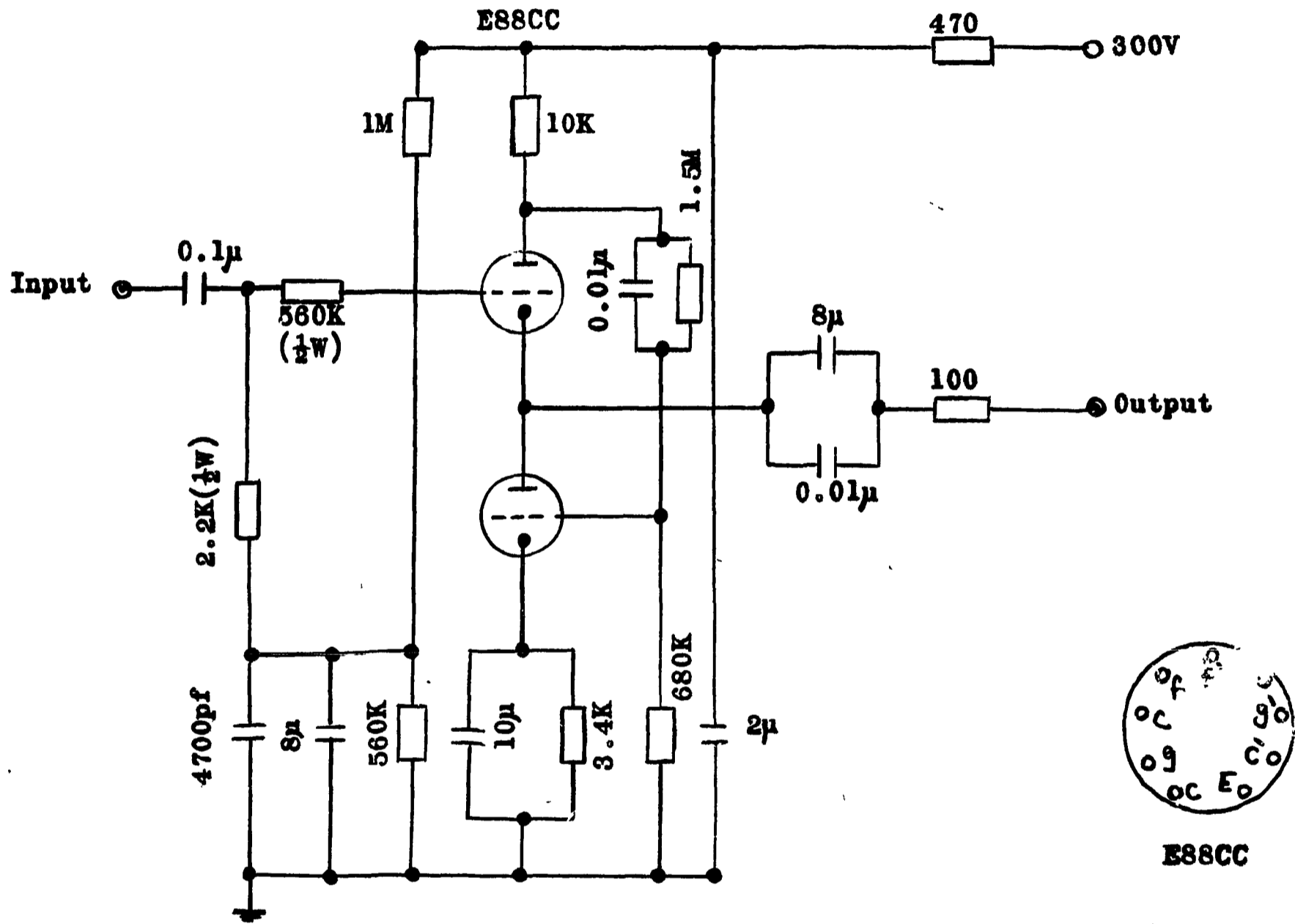


Fig. (11): Matching Cathode Follower.

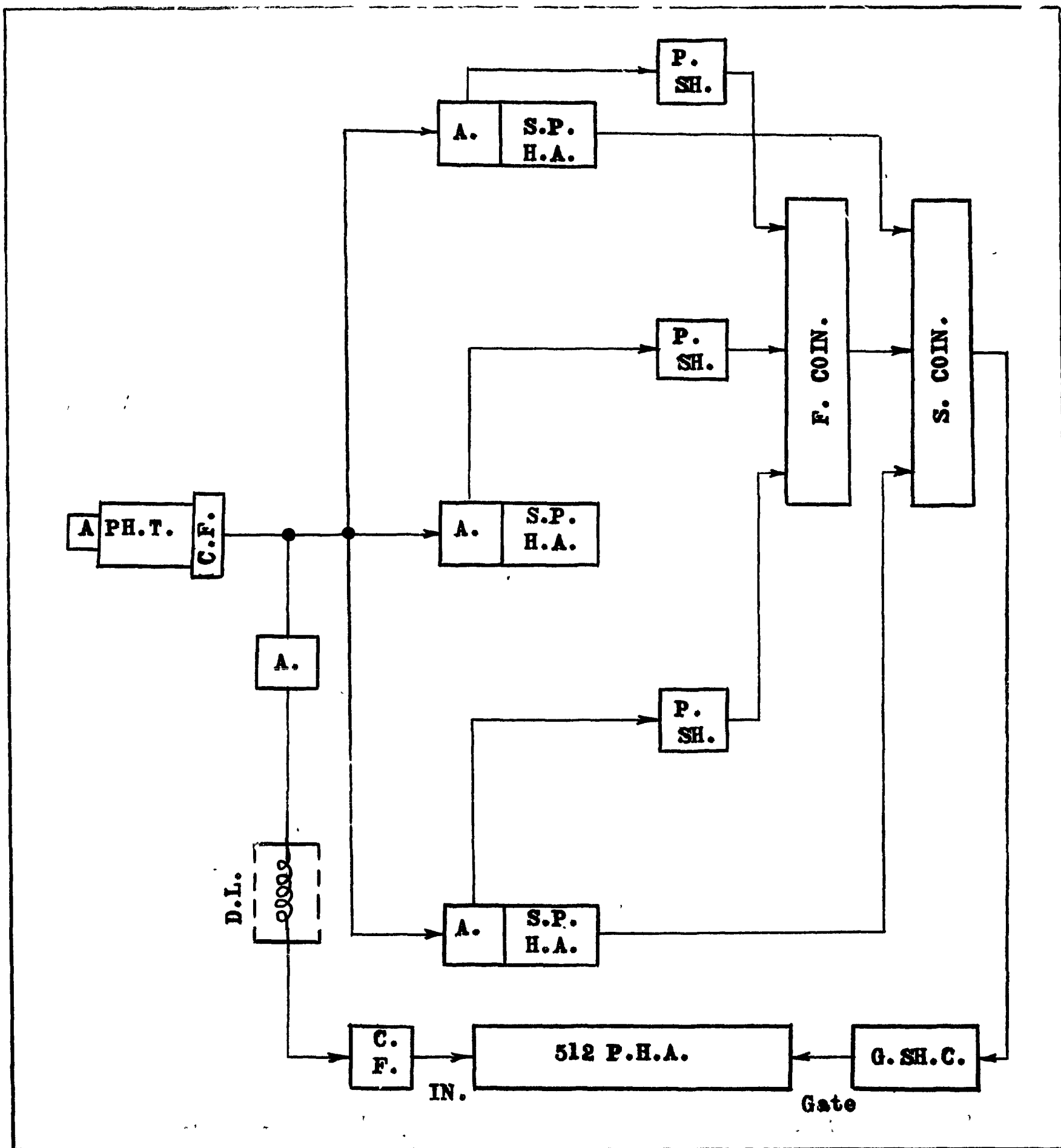


Fig. (12): Arrangement for Checking the Fast-Slow Coincidence System.

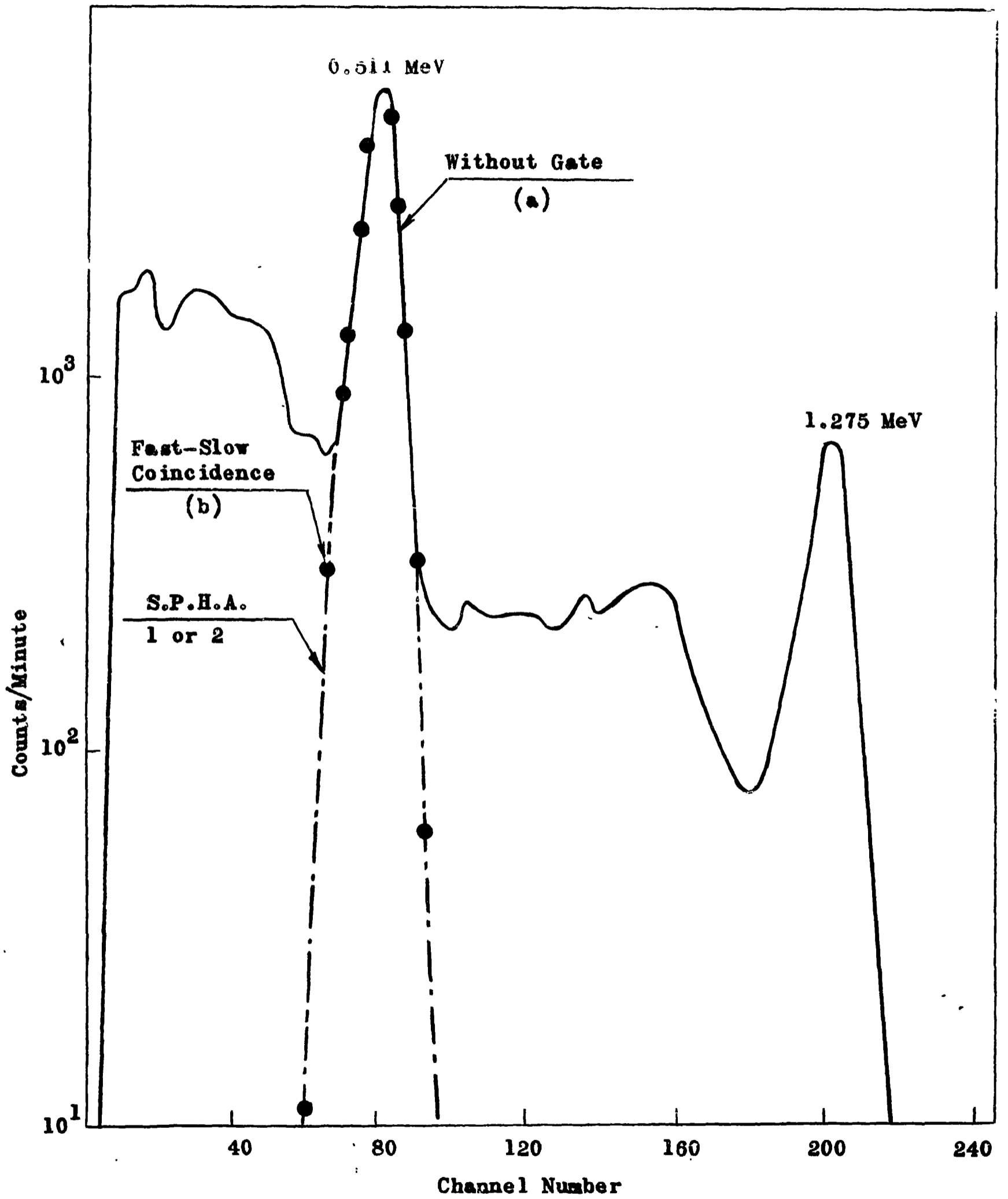


Fig. (13a,b): Na^{22} Spectrum by Fast-Slow Coincidence System.

when the gate was used which represent nearly the total area of the annihilation photo-peak.

This was carried out for the second side detector B and the spectra were found the same for both crystal systems within the standard error.

This indicates that the electronic equipment are satisfactory for a three-crystal pair spectrometer.

7. THERMAL NEUTRON CAPTURE GAMMA-RAYS IN NATURAL LEAD

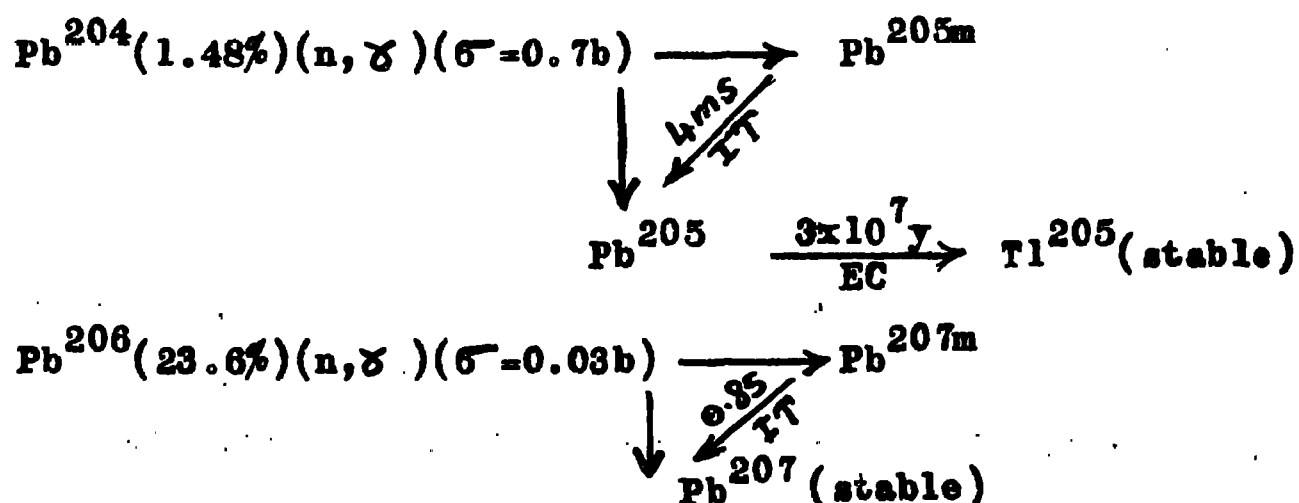
7.1 Introduction :

The study of thermal neutron capture gamma-rays emitted by lead was aimed at first to investigate the pair spectrometer peak shape at the gamma-rays of energy 7.38 MeV. The spectrum obtained could be compared with Adyasevich et al.⁽⁹⁾ and Kinsey et al.^(10,11) results, as a check for our pair spectrometer working function.

The lead sample consisted of (22,04 gm) of chemically pure lead 99.9%, 1.2 cm in diameter and 2 cm thick, was placed in the external thermal neutron beam with its axis extending along the neutron beam.

The arrangement of counters was as shown in Fig. (1), with the lead cylindrical center at a distance 4 cm from the front surface of central crystal.

The abundances and cross-section of each of the four stable isotopes of lead are as follows^(12,13)



$\text{Pb}^{207}(22.6\%)(n, \gamma) \text{Pb}^{208}(\sigma = 0.72\text{b})$ stable.

$\text{Pb}^{208}(52.3\%)(n, \gamma) \text{Pb}^{209}(\sigma = 0.5\text{mb}) \xrightarrow{\beta^-} \text{Bi}^{209}$ (stable)

Effective capture cross-section is :

$$\sigma_c(2200) = (0.172 \pm 0.002)\text{b}$$

This cross-section has been normalized to a value of; $\sigma_a(2200) = 771\text{b}$ for Harwell standard boron instead of the value of 766.6 b they used.

Kinsey et al.^(10,11) studied the lead neutron capture gamma-ray spectrum by a pair spectrometer. Only two strong gamma-rays have been detected during the bombardment with thermal neutrons. The weaker of the two is due to capture in Pb^{206} and has an energy of $6.734 \text{ MeV} \pm 0.008 \text{ MeV}$, and the stronger is due to capture in Pb^{207} and has an energy $7.380 \text{ MeV} \pm 0.008 \text{ MeV}$. Apart from a very weak gamma-ray with an energy of $6.90 \pm 0.05 \text{ MeV}$, no other radiation has been detected.

The 6.90 MeV gamma-ray may be due to the excitation of a hitherto unknown state in Pb^{208} or it may be due to an impurity.

In (1961) Journey et al.⁽¹⁴⁾, by the aid of the Compton spectrometer, found the gamma-rays of 7.370 and 6.740 MeV due to $\text{Pb}^{207}(n, \gamma)\text{Pb}^{208}$ and $\text{Pb}^{206}(n, \gamma)\text{Pb}^{207}$ to have an intensity ratio 10 ± 1 for natural lead in agreement with previous work^(11,12). If no other gamma-ray transitions occur for these reactions then the observed intensity ratio should correspond to the absorption cross-section. Ten weak gamma-rays are observed between 2.5 and 6.7 MeV. but their total intensity can not alter the $\text{Pb}^{207}/\text{Pb}^{206}$ capture ratio to be greater than 13. File oscillator absorption cross-section measurements give a capture ratio of 27 ± 5 for natural lead⁽¹⁵⁾. Only one of the observed weak lines (2.617) MeV shows any simple correlation with known excited states in lead. The remaining nine weak lines might be due to impurities. A theoretical estimate of transitions to the first excited state of Pb^{207} is 0.3 for direct capture⁽¹⁶⁾.

In (1962) Motz et al.⁽¹⁷⁾ observed with the high energy resolution Compton spectrometer spectra resulting from slow neutrons capture in natural and radiogenic lead targets.

Spectra from similar targets and from samples of enriched Pb^{204} , Pb^{206} , Pb^{207} and Pb^{208} have been observed with a three scintillation pair spectrometer.⁽¹⁷⁾

A transition of 6.472 MeV is assigned to $\text{Pb}^{204}(\text{n}, \gamma)\text{Pb}^{205}$ and is believed to excite the corresponding $(f_{5/2})^2 P_{3/2}$ three hole state of Pb^{205} . Its intensity is 0.2 of the ground state transition and results in an excited level of 265 keV in Pb^{205} .

The sum of $\text{Pb}^{204}(\text{n}, \gamma)$ lines results in a minimum total capture cross-sections of 420 mb for Pb^{204} . Twenty-one transition for $\text{Pb}^{204}(\text{n}, \gamma)\text{Pb}^{205}$ have been observed and expected to be transitions between low spin states of Pb^{205} .

In (1965) Greenwood et al.⁽¹³⁾ using NaI(Tl) scintillation crystal spectrometer observed the 7.38 MeV gamma-ray energy due to thermal neutron capture in Pb^{207} isotope which accounts for about 90% of the thermal neutron absorption in a sample of natural Pb.

In (1967) Journey and Motz⁽¹⁸⁾ observed the gamma-ray spectrum following thermal neutron capture by $\text{Pb}^{204}(\text{n}, \gamma)\text{Pb}^{205}$ using Li-drifted Ge detector placed at the centre of cylindrical NaI(Tl) annulus. The target contains Pb^{204}

74.1% Pb^{204} , 11.8% Pb^{206} , 5.9% Pb^{207} , 8.2% Pb^{208}

The high energy neutron capture gamma-rays observed from $\text{Pb}^{204}(\text{n}, \gamma)\text{Pb}^{205}$ were 16 lines from 3.5720 MeV to 6.7315 MeV and the low energies were 24 lines from 2.1170 MeV till 0.2269 MeV. Taking into consideration that the binding energy $B_n = 6.7342$ MeV in Pb^{205} , the neutron capture cross-section for Pb^{204} was found 661 ± 70 mb.

7.2 Experimental Results and Discussion :

The spectrum of lead capture gamma-rays obtained uncorrected for background is shown in Fig. (14). It is clearly that the two characteristic peaks at 7.38 MeV and 6.74 MeV are in agreement with Kinsey et al.⁽¹⁰⁾, Ad'yasivich et al.⁽⁹⁾ and Motz et al.⁽¹⁷⁾.

The good resolution of the spectrometer can be seen from the growth of the peak number (2) with energy 6.92 MeV which has been observed by Kinsey et al.⁽¹⁰⁾.

The figure shows also an evidence for the presence of another gamma-ray peak number (4) with an energy of 6.47 MeV which has been reported by Motz et al.⁽¹⁷⁾ where it has been assigned to Pb^{205} .

Few weak gamma-rays are observed at the low energy end of the spectrum Fig. (14). The most pronounced peaks of them have energies 2.95, 2.62, 2.12, 1.80 and 1.65 MeV. Most of these observed weak lines show simple correlation with known excited states in lead^(18,19,20).

The background form is quite satisfactory for the pair crystal spectrometer in an external neutron beam. The resolution of the 7.38 MeV peak was found 2.6% which is far better than the single crystal spectrometer.

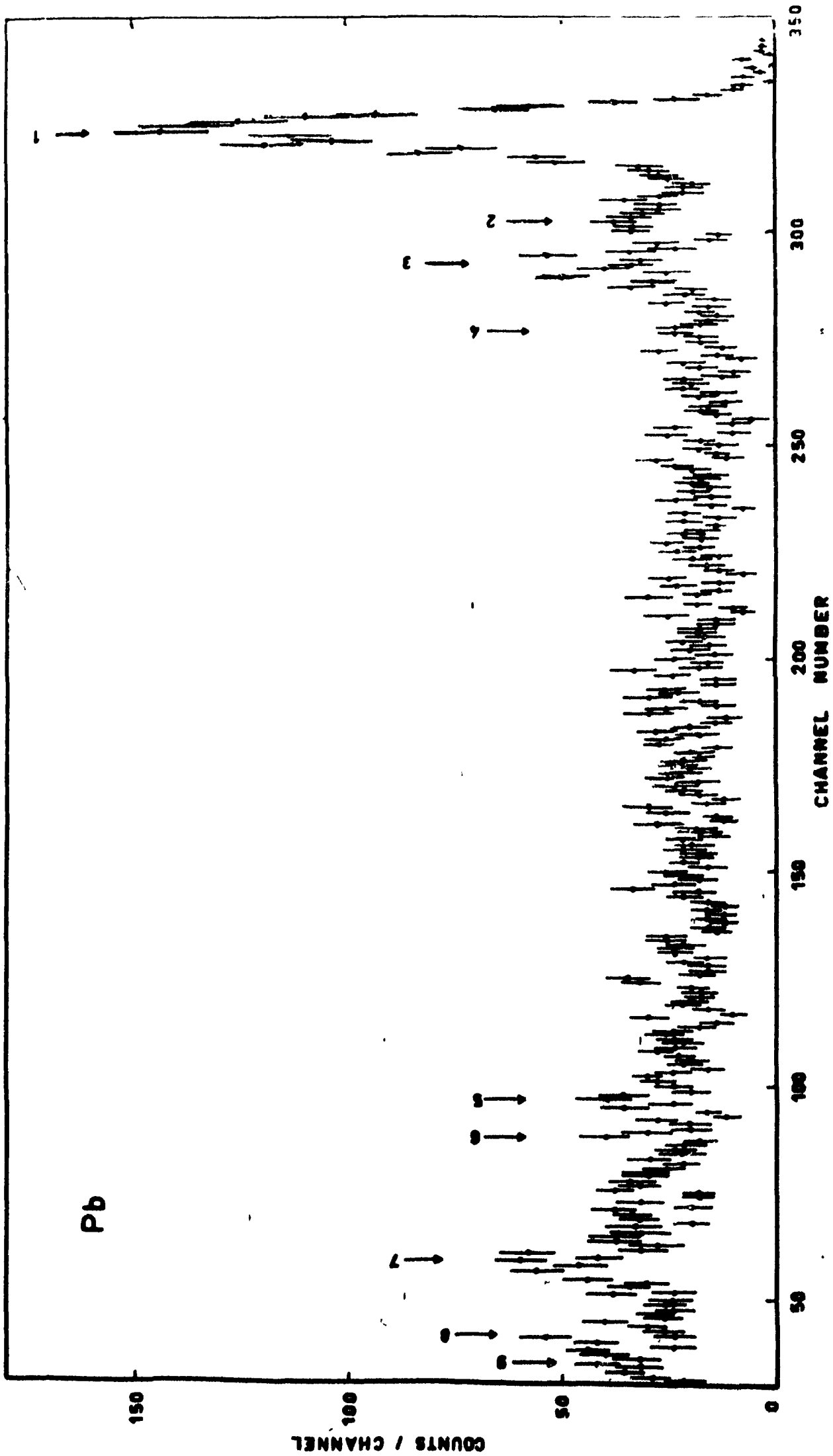


Fig. (14) PAIR SPECTROMETER SPECTRUM OF CAPTURE GAMMA RAYS FROM A NATURAL LEAD SAMPLE (UNCORRECTED)

ACKNOWLEDGMENT

The authors wish to express their thanks to Professor I. Hamouda, Head of the Reactor and Neutron Physics Department, U.A.R.A.E.E., for his interest in this work, for his useful discussions and for offering all the possible facilities throughout the experimental work.

The authors wish to express their thanks to Professor M. El-Nadi, Head of Physics Department, Cairo University for his interest in this work, for his helpful advice and continuous guidance.

R E F E R E N C E S

- (1) H.M. Abu-Zeid and A.M. Hassan, U.A.R.A.E.E./Rep.-93, (1970).
- (2) Vegors, S.H., Jr., Marsden, L.L. and Heath, R.L., Calculated Efficiencies of Cylindrical Radiation Detectors, A.E.C., Research and Development Report, IDO-16370 (Sept. 1, 1958).
- (3) Inglis, D.R., Phys. Rev., 74, 1876 (1948); 81, 914 (1951).
- (4) Robert, W. Landee, Donoranc, Daris, Al-Bert P. and Al-Brecht, McGraw-Hill Book Company, Electronic Designers Handbook, Inc., 36110 Sec. (3) and Sec. (15), (1957).
- (5) Vin Zeiuff and John Markus, McGraw-Hill Book Company, Inc., Electronics Manual for Radio Engineers, Chapter III and X , (1949).
- (6) Kai Sigbahn, Beta and Gamma-ray Spectroscopy, Chapter XVIII, (1955).
- (7) Elmore and Sands, "Electronics", McGraw-Hill, New York, (1949).
- (8) Heath, R.L., Scintillation Spectrometry Gamma-ray Spectrum catalogue., IDO-16980-2 AEC Research and Development Report Physics TID-1500 (31STE), ISSUED, August (1964).
- (9) Ad'yasevich B.P., Groshev, L.V. and Demidov, A.M., Atom. Energy, 1(2) 40 (1956), Journal of Nuclear Energy 3, 258 (1966), Soviet Journal of Atomic Energy 1, 183 (1956).
- (10) Kinsey, B.B., Bartholomew, G.A., and Walker, W.H., Phys. Rev., 78, 77 (1950).
- (11) Kinsey, B.B., Bartholomew, G.A., and Walker, W.H., Phys. Rev., 82, 380 (1951).
- (12) Groshev, L.V. and Demidov, A.M., Lutsenko, V.N. and Pelekhev, V.I., Atlas of Gamma-rays Spectra from Radiative Capture of Thermal Neutrons, Pergamon Press London, (1959).

- (13) Greenwood, R.C., and Reed, J.H., Prompt Gamma-rays from Radiative Capture of Thermal Neutrons, Vol. 1 and 2 II, TR-666, Technology Center II T. Res. Inst. Chicago, Illinois, (1965).
- (14) Journey, E.T., Carter, R.E. and Motz, H.T., Bull. Am. Phys. Soc., 6, 62, (1961).
- (15) Aitken A., Proc. Phys. Soc., (London) A. 65, 761, (1952).
- (16) Lane, A.M. and Lynn, J.E., Nucl. Phys., 17, 586, (1960).
- (17) Motz, H.T., Journey, E.T., and Carter, R.E., Los Alamos Sc. Lab. Bull. Am. Phys. Soc., 7, 11, (1962).
- (18) Journey, E.T. and Motz, H.T., Nucl. Phys. A., 94, 351, (1967).
- (19) Rothmann, M.A. and Mandeville, C.E., Phys. Rev., 93, 796, (1954).
- (20) Day, B., Phys. Rev., 102, 767, (1956).